

Lyapounov exponent and density of states of a one-dimensional non-Hermitian Schrödinger equation

Bernard Derrida*, Jesper Lykke Jacobsen* and Reuven Zeitak†

**Laboratoire de Physique Statistique¹,*

Ecole Normale Supérieure,

24 rue Lhomond, F-75231 Paris CEDEX 05, FRANCE.

† Department of Chemical Physics,

The Weizmann Institute of Science,

Rehovot 76100, ISRAEL.

ABSTRACT

We calculate, using numerical methods, the Lyapounov exponent $\gamma(E)$ and the density of states $\rho(E)$ at energy E of a one-dimensional non-Hermitian Schrödinger equation with off-diagonal disorder. For the particular case we consider, both $\gamma(E)$ and $\rho(E)$ depend only on the modulus of E . We find a pronounced maximum of $\rho(|E|)$ at energy $E = 2/\sqrt{3}$, which seems to be linked to the fixed point structure of an associated random map. We show how the density of states $\rho(E)$ can be expanded in powers of E . We find $\rho(|E|) = \frac{1}{\pi^2} + \frac{4}{3\pi^3}|E|^2 + \dots$. This expansion, which seems to be asymptotic, can be carried out to an arbitrarily high order.

PACS numbers: 03.65.-w, 02.50.Ng, 74.40.+k, 31.15.Md

Keywords: Non-Hermitian quantum mechanics, density of states, invariant distribution, localisation.

Submitted to J. Stat. Phys.

¹Laboratoire associé aux Universités Paris 6, Paris 7 et au CNRS.

1 Introduction

It has been realised over the last few years that a number of non-equilibrium problems can be described through the time evolution of a non-Hermitian random Hamiltonian. Some noteworthy applications include the motion of a particle in an imaginary vector potential [1], vortex line pinning in superconductors [2, 3], and growth models in population biology [4]. The interest for non-Hermitian random Schrödinger equations increased further [5, 6, 7, 8, 9, 10, 11, 12] as it was realised that, at least in some cases, a transition from localised to delocalised states could take place even in one dimension.

The simplest examples considered were one-dimensional tight-binding models for which the wave function satisfies

$$e^h\psi_{n+1} + e^{-h}\psi_{n-1} + V_n\psi_n = E\psi_n, \quad (1.1)$$

where V_n is a random potential at site n and E is the energy. For real h and periodic boundary conditions ($n \equiv N + n$), it was shown [1, 5] that the eigenvalues are located (for a large system size) either on the real axis, or on lines which can be understood from the knowledge of the Lyapounov exponent for $h = 0$.

Here we consider another simple one-dimensional non-Hermitian Schrödinger equation, first introduced by Feinberg and Zee [3]:

$$e^{i\theta_n}\psi_{n+1} + e^{i\chi_n}\psi_{n-1} = E\psi_n. \quad (1.2)$$

In this case there is no random potential V_n , and the disorder is purely off-diagonal. Both θ_n and χ_n are uniformly distributed between 0 and 2π , and they are all independent.

A numerical study [3] of the spectrum of this Schrödinger equation suggested that the density of states was roughly uniform in a circle of radius $\sim \pi/2$. We found it challenging to see whether existing tools [13, 14, 15, 16] could be used to calculate this spectrum.

In the present work we mostly study the density of states of Eq. (1.2) by calculating the associated Lyapounov exponent and using the Thouless formula [17] (which remains valid for non-Hermitian one-dimensional models as shown in Section 2).

The calculation of the Lyapounov exponent, and consequently the density of states, can be done either by Monte Carlo methods or by solving numerically an integral equation

for the Ricatti variable $r_n = |\psi_n/\psi_{n-1}|$. This is done in Section 3, where we also discuss the possibility of singularities both in the probability distribution of r_n and in the density of eigenvalues E of Eq. (1.2).

In Section 4 we develop a method to perturbatively calculate the Lyapounov exponent and the density of states, in powers of the energy E . This approach is an extension of similar calculations done in the past, where the anomalous behaviour of the density of states at the band centre was obtained in the Hermitian case [15, 16]. Our expansion indicates that the radius of convergence is $E = 0$ and that the series is asymptotic.

2 The Lyapounov exponent and the density of states

An old and powerful way [13, 14] of studying one-dimensional random systems consists in rewriting recursion formulae like Eqs. (1.1)–(1.2) in a matrix form. Indeed, Eq. (1.2) can be recast as

$$\begin{bmatrix} \psi_{n+1} \\ \psi_n \end{bmatrix} = M_n \begin{bmatrix} \psi_n \\ \psi_{n-1} \end{bmatrix}, \quad (2.1)$$

where M_n is a random 2×2 matrix

$$M_n(E, \theta_n, \chi_n) = \begin{bmatrix} Ee^{-i\theta_n} & -e^{i(\chi_n - \theta_n)} \\ 1 & 0 \end{bmatrix}, \quad (2.2)$$

so that for any choice of the energy E and of the wave function ψ_0 and ψ_1 at sites 0 and 1, the wave function ψ_n for $n \geq 2$ reads

$$\begin{bmatrix} \psi_{n+1} \\ \psi_n \end{bmatrix} = \prod_{p=1}^n \begin{bmatrix} Ee^{-i\theta_p} & -e^{i(\chi_p - \theta_p)} \\ 1 & 0 \end{bmatrix} \begin{bmatrix} \psi_1 \\ \psi_0 \end{bmatrix}. \quad (2.3)$$

If ψ_0 and ψ_1 are chosen arbitrarily (*i.e.* they are fixed, and not tuned functions of E and of all the θ_p and χ_p), one expects that for large N

$$\lim_{N \rightarrow \infty} \frac{1}{N} \log |\psi_N| = \gamma(E), \quad (2.4)$$

where $\gamma(E)$ is the largest Lyapounov exponent of the product of random matrices (2.3).

Because the matrices M_n are invariant under the transformation $M_n(E, \theta_n, \chi_n) \rightarrow M_n(Ee^{i\beta}, \theta_n + \beta, \chi_n + \beta)$ for any β , and because by shifting all the phases θ_n and χ_n by

a constant β one gets an equally likely random sample, it is clear that $\gamma(E) = \gamma(Ee^{i\beta})$. Thus the Lyapounov exponent depends only on the modulus of E . For similar reasons, the average density $\rho(E)$ of eigenvalues is invariant under the change $E \rightarrow Ee^{i\beta}$:

$$\begin{aligned}\gamma(E) &= \gamma(|E|), \\ \rho(E) &= \rho(|E|).\end{aligned}\tag{2.5}$$

In fact these two quantities are related by the Thouless formula [17]

$$\gamma(E) = \int_{-\infty}^{\infty} dE_x \int_{-\infty}^{\infty} dE_y \rho(E_x + iE_y) \log |E - (E_x + iE_y)|,\tag{2.6}$$

which can be derived as in the Hermitian case by the following argument: Consider a finite system of N sites with Dirichlet boundary conditions ($\psi_0 = \psi_{N+1} = 0$). If one fixes $\psi_0 = 0$ and $\psi_1 = 1$, the ψ_{N+1} calculated from the recursion (2.1) is found to be a polynomial of degree N in E , the zeroes of which are the N eigenvalues E_α (for Dirichlet boundary conditions):

$$\psi_{N+1}(E) = \exp\left(-i \sum_{n=1}^N \theta_n\right) \prod_{\alpha=1}^N (E - E_\alpha).\tag{2.7}$$

Applying Eq. (2.4) for large N leads to Eq. (2.6).

It turns out that for all $E \neq 0$, the Lyapounov exponent $\gamma(E)$ is strictly positive by the Furstenberg theorem [18, 19]. (This will in fact be confirmed by our numerical results, and by the small- E expansion of Section 4.) One can then argue that the density of states is independent of the boundary conditions. Indeed, for general E , Dirichlet ($\psi_{N+1}(E) = \psi_0(E) = 0$) and periodic boundary conditions ($\psi_{N+1}(E) = \psi_1(E)$) are very similar: Both require that $\psi_{N+1}(E) \sim e^{N\gamma(E)}$, obtained by iterating Eq. (2.3), takes very untypical small values at the eigenenergies. Thus, the eigenvalues corresponding to respectively periodic and Dirichlet boundary conditions should be very close, their distance being typically exponentially small in N .

The Thouless formula (2.6) can be inverted by using an analogy with two-dimensional electrostatics. If we interpret $\gamma(E)$ in Eq. (2.6) as the two-dimensional Coulomb potential created by a charge density $\rho(E')$, it follows from Poisson's equation that

$$\rho(E_x + iE_y) = \frac{1}{2\pi} \left(\frac{\partial^2}{\partial E_x^2} + \frac{\partial^2}{\partial E_y^2} \right) \gamma(E_x + iE_y),\tag{2.8}$$

or, exploiting the rotational symmetry of $\gamma(E)$ and of $\rho(E)$, that

$$\rho(|E|) = \frac{1}{2\pi} \left(\frac{d^2}{d|E|^2} + \frac{1}{|E|} \frac{d}{d|E|} \right) \gamma(|E|). \quad (2.9)$$

For $|E| > 2$ the density of states vanishes. To see this, consider an eigenfunction ψ_n corresponding to an eigenvalue E_α . By applying the triangular inequality to Eq. (1.2), one obtains $|E_\alpha \psi_n| \leq |\psi_{n-1}| + |\psi_{n+1}|$. Choosing n such that $|\psi_n| = \max(|\psi_i|)_{i=1}^N$, this implies $|E_\alpha| \leq 2$. As the density of states $\rho(E)$ vanishes for $|E| > 2$, by expanding the logarithm in Eq. (2.6) and by using the rotational symmetry (2.5) of $\rho(E)$ one readily finds that

$$\gamma(E) = \log |E| \quad \text{for} \quad |E| > 2. \quad (2.10)$$

All our calculations which follow are based on another reformulation of Eq. (1.2). Introducing the Ricatti variable r_n

$$r_n = \left| \frac{\psi_n}{\psi_{n-1}} \right| \quad (2.11)$$

the problem (2.3) takes on the form of iterating a random map shown in Figure 1

$$r_{n+1} = \left| \frac{1}{r_n} + E e^{i\varphi_n} \right|, \quad (2.12)$$

where φ_n (which is equal to $\chi_n - \theta_n + \pi$ modulo 2π) is uniformly distributed between 0 and 2π . The Lyapounov exponent is then given by

$$\gamma(E) = \lim_{N \rightarrow \infty} \frac{1}{N} \sum_{n=1}^N \log r_n. \quad (2.13)$$

For large n the probability distribution of r_n becomes independent of n , and the invariant distribution $P(r, E)$ satisfies

$$P(r, E) = \int_0^{2\pi} \frac{d\varphi}{2\pi} \int_0^\infty ds P(s, E) \delta \left(r - \left| \frac{1}{s} + E e^{i\varphi} \right| \right). \quad (2.14)$$

From the knowledge of this invariant distribution, the calculation of the Lyapounov exponent $\gamma(E)$ follows from Eq. (2.13), and one has

$$\gamma(E) = \int_0^\infty dr P(r, E) \log r, \quad (2.15)$$

whereas the density of states $\rho(E)$ is given by Eq. (2.9).

All the rest of the paper is devoted to the determination of the invariant distribution $P(r, E)$ solving Eq. (2.14), and to the calculation of the Lyapounov exponent $\gamma(E)$ as well as the density of states $\rho(E)$.

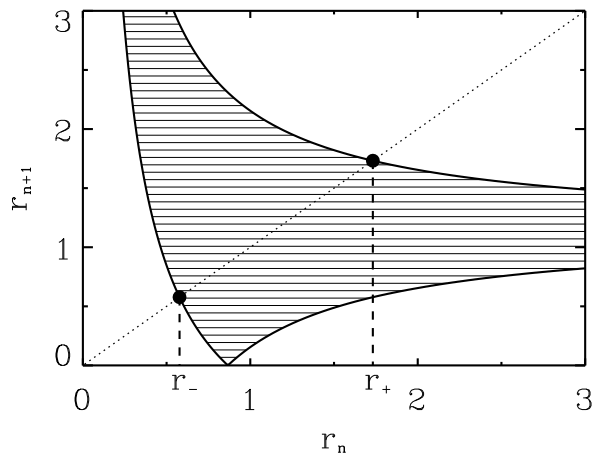


Figure 1: Schematical illustration of the random map (2.12). Given r_n , its iterate r_{n+1} is randomly distributed in the hatched region. The boundary constitutes two maps, T_+ and T_- , obtained from Eq. (2.12) by choosing $\varphi_n = 0$ and $\varphi_n = \pi$ respectively. For $E < 2$, these maps possess fixed points $r_+ = T_+(r_+)$ and $r_- = T_-(r_-)$, that are respectively attractive and repulsive. For the particular energy $E = 2/\sqrt{3}$ chosen on the figure, $T_-(r_+) = r_-$.

3 Numerical study

In this section we numerically determine the invariant distribution $P(r, E)$ solution of Eq. (2.14), the Lyapounov exponent $\gamma(E)$, and the density of states $\rho(E)$.

According to Eq. (2.9) the computation of the density of states requires both $\gamma(E)$ and its first two derivatives. Whilst $\gamma(E)$ is rather easy to determine numerically, a precise estimate of its derivatives with respect to the energy turns out to be far more difficult. We have attacked the problem by two different methods.

3.1 The Monte Carlo approach

This first method consists in iterating Eq. (2.12) for a large sample. Typical shapes obtained for the stationary distribution $P(r, E)$ are shown in Figure 2.

First, one notices that depending on the value of E , the support of the invariant measure $P(r, E)$ is either finite or infinite. If one assumes that the support is an interval $[r_{\min}, r_{\max}]$, we see from Eq. (2.12) that if $r_n \in [r_{\min}, r_{\max}]$, the requirement that also $r_{n+1} \in [r_{\min}, r_{\max}]$ gives conditions that r_{\min} and r_{\max} should satisfy. After analysing all the possible cases, one finds that the support of the distribution $P(r, E)$ is the whole positive real axis for $E < 2$, whereas for $E > 2$ the support is finite, with r_{\min} and r_{\max} satisfying $r_{\min} = E - 1/r_{\min}$ and $r_{\max} = E + 1/r_{\min}$, that is

$$r_{\min} = \frac{1}{2} \left(E + \sqrt{E^2 - 4} \right), \quad r_{\max} = \frac{1}{2} \left(3E - \sqrt{E^2 - 4} \right). \quad (3.1)$$

Second, for large enough E , there are apparent singularities at certain values of r . These singularities seem to be remarkable points of the maps T_+ and T_- obtained from Eq. (2.12) by choosing $\varphi_n = 0$ or $\varphi_n = \pi$, *i.e.*

$$\begin{aligned} T_+(r) &= E + \frac{1}{r}, \\ T_-(r) &= \left| E - \frac{1}{r} \right|. \end{aligned} \quad (3.2)$$

For each value r_n , it is easy to see that $T_+(r_n)$ and $T_-(r_n)$ are the two extreme values that r_{n+1} can take: $T_-(r_n) \leq r_{n+1} \leq T_+(r_n)$.

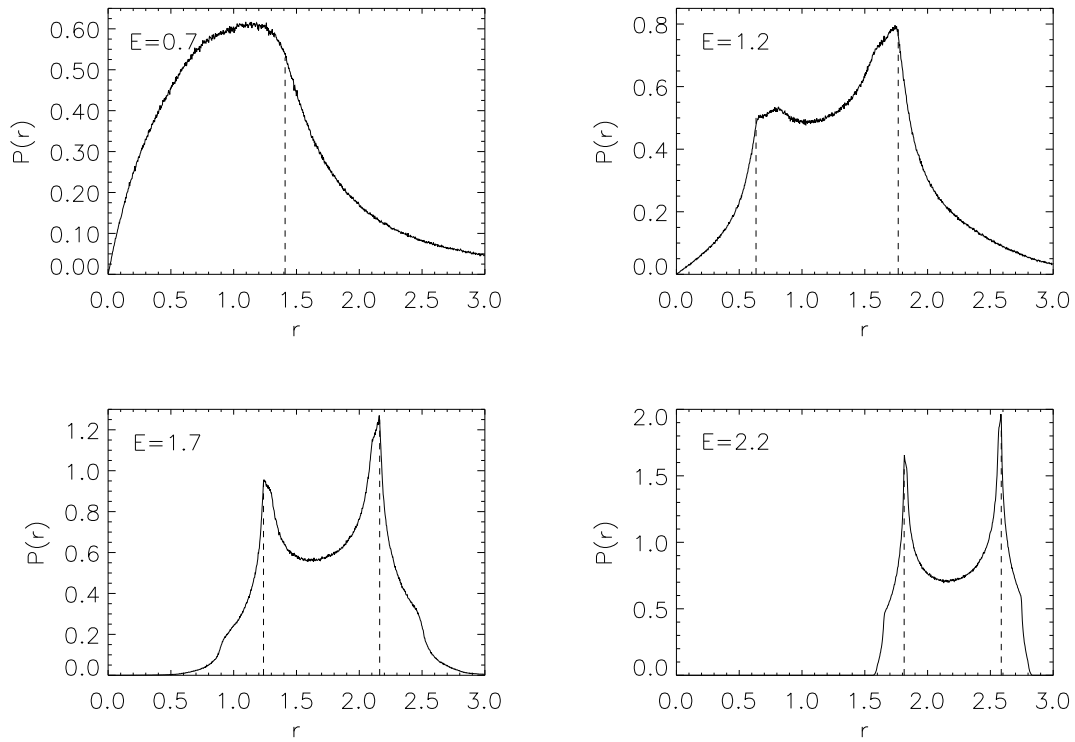


Figure 2: Histograms of r_n for energies $E = 0.7, 1.2, 1.7$ and 2.2 , obtained using $N = 10^7$ iterations. Apparent singularities occur at the points r_+ and $T_-(r_+)$, marked by dashed lines on the figure.

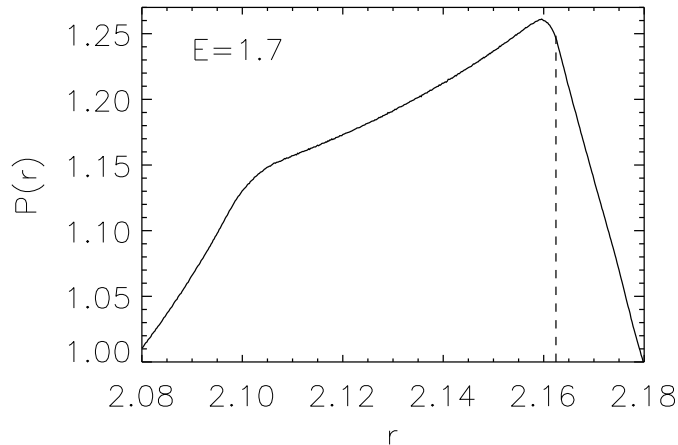


Figure 3: Close-up of the most visible “singularity” of Figure 2.c, this time using $N = 10^{11}$ iterations.

The fixed point of T_+

$$r_+ = \frac{1}{2} \left(E + \sqrt{E^2 + 4} \right) \quad (3.3)$$

coincides with the most visible singularity of $P(r, E)$ in Figure 2, whereas the iterate $T_-(r_+)$ gives the position of another very visible singularity of $P(r, E)$. Other apparent singularities seem to be located at the points $T_-^2(r_+)$ and $T_+(T_-(r_+))$.

In Appendix A, we show that the singularities in $P(r, E)$ are, if at all present, much weaker than they look on Figure 2. This is confirmed by Figure 3, which is an enlargement of Figure 2.c, where there is a clear rounding of the singularity at r_+ .

The calculation of the Lyapounov exponent is straightforward by Monte Carlo methods. One just iterates the random recursion (2.12) a large number N of times (typically $N = 10^8$) and one obtains $\gamma(E)$ by

$$\gamma(E) \simeq \frac{1}{N} \sum_{n=N'}^{N+N'} \log r_n \quad (3.4)$$

where N' is a large enough number of iterations to eliminate the transient effects due to the initial choice of r_0 (here we took $N' = N/10$ which is exceedingly sufficient).

For the density of states one needs Eq. (2.9) to calculate the first two derivatives of $\gamma(E)$ with respect to E . A possible approach would be to measure $\gamma(E)$ from Eq. (3.4)

for three nearby energies, $E - \Delta E$, E , and $E + \Delta E$, and calculate numerically the first and second derivatives. With this method it is however hard to find a good compromise for the choice of ΔE : If ΔE is too small, one does not have enough precision on the derivatives, and if ΔE is too large, all the structure of the density of states is artificially smoothed.

To avoid this difficulty we tried to iterate directly the derivatives of r_n with respect to E . The recursion (2.12) has the form

$$r_{n+1} = f_0(r_n, E, \varphi_n). \quad (3.5)$$

Now, if $r_n^{(1)}$ and $r_n^{(2)}$ denote the first and the second derivatives of r_n with respect to E , one can obtain (in a complicated form which we do not reproduce here because we wrote it in our programmes through a change of variables) recursion formulae for these derivatives

$$r_{n+1}^{(1)} = f_1(r_n, r_n^{(1)}, E, \varphi_n), \quad (3.6)$$

$$r_{n+1}^{(2)} = f_2(r_n, r_n^{(1)}, r_n^{(2)}, E, \varphi_n). \quad (3.7)$$

Iterating these recursions N times yields an estimate for the first two derivatives of $\gamma(E)$

$$\begin{aligned} \frac{d\gamma(E)}{dE} &\simeq \frac{1}{N} \sum_{n=N'}^{N+N'} \frac{r_n^{(1)}}{r_n}, \\ \frac{d^2\gamma(E)}{dE^2} &\simeq \frac{1}{N} \sum_{n=N'}^{N+N'} \left[\frac{r_n^{(2)}}{r_n} - \left(\frac{r_n^{(1)}}{r_n} \right)^2 \right]. \end{aligned} \quad (3.8)$$

Figure 3 shows our results for $\gamma(E)$ and $\rho(E)$ obtained by this Monte Carlo approach. Whilst the results for $\gamma(E)$ seem to be alright, the density of states exhibits some irregularities. We tried to understand the origin of these irregularities by changing the length N of the sample, the generator of random numbers, and the way in which Eqs. (3.6)–(3.7) were parametrised in our programmes. Although the positions of the irregularities were observed to change, we were unable to eliminate them altogether. Nevertheless we believe that they do have a purely numerical origin: From time to time, there is a very small value of r_n produced by the iteration of Eqs. (3.5)–(3.7), and this gives such a huge contribution to the sums (3.8) that all the remaining terms become negligible. Usually this big contribution is followed at the next step by another huge contribution of opposite

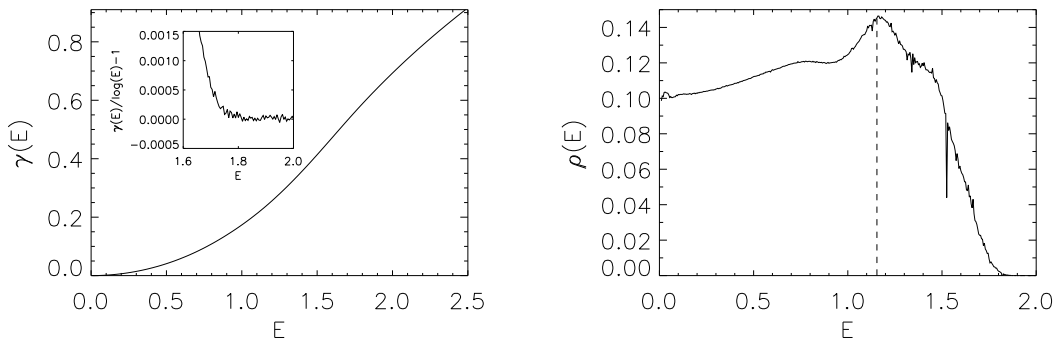


Figure 4: Lyapunov exponent $\gamma(E)$ and density of states $\rho(E)$ obtained by Monte Carlo after 10^8 iterations. The inset in the left part of the figure shows the asymptotic approach to the exact result (2.10). In figure 4b, the vertical dashed line indicates the energy $E = 2/\sqrt{3}$.

sign which more or less compensates the first big contribution. These events (where r_n is very small) have a dramatic effect on the accuracy of our results, with the unfortunate consequence that the more we iterate, the more of these events we see, so that the more irregularities are visible.

We unfortunately could not find a satisfactory way of avoiding these difficulties, and so we tried a completely different approach discussed in the next subsection.

In Figure 4.b, we see that the density of states $\rho(E)$ exhibits a non-trivial structure with a pronounced maximum at an energy $E \simeq 1.15$. Trying to understand the origin of this maximum, we realised that at energy

$$E = \frac{2}{\sqrt{3}} \simeq 1.1547 \dots \quad (3.9)$$

the point $T_-(r_+)$ becomes a fixed point of T_- . In a more physical language, if one considers an infinite sample for which

$$\begin{aligned} \theta_n &= 0 \quad \text{and} \quad \chi_n = \pi \quad \text{for} \quad n < 0, \\ \theta_n &= 0 \quad \text{and} \quad \chi_n = 0 \quad \text{for} \quad n = 0, \\ \theta_n &= \pi \quad \text{and} \quad \chi_n = 0 \quad \text{for} \quad n > 0, \end{aligned} \quad (3.10)$$

one finds that there is a bound state at energy $E = 2/\sqrt{3}$ corresponding to a wave function $\psi_n \propto 3^{-|n|/2}$ in addition to the continuous part of the spectrum at imaginary energies, $E = ix$ with $-2 \leq x \leq 2$.

We believe that the origin of the sharp maximum in $\rho(E)$ at energy $E = 2/\sqrt{3}$ is due to the existence of these bound states, as in the case of impurity bands for Hermitian problems [19, 20]. We did not succeed, however, to determine whether the density of states is analytic at this special energy $E = 2/\sqrt{3}$, or whether it presents some weak non-analyticity.

Our numerical results for $\gamma(E)$ in Figure 4.a can be fitted for small E by an expression of the form

$$\gamma(E) = k_1 E^2 + k_2 E^4 + \dots \quad (3.11)$$

with $k_1 = 0.1595 \pm 0.0005$ and $k_2 = 0.017 \pm 0.001$. To be more precise, we first find k_1 as the extrapolated interception of $\gamma(E)/E^2$ with the ordinate. Then, subtracting the $k_1 E^2$ term, k_2 can be similarly found from the residual E^4 dependence. Needless to say, this procedure greatly enhances numerical noise at each stage, and so we had to content ourselves finding the first two terms. These are in good agreement with the results $k_1 = \frac{1}{2\pi} \simeq 0.1592$ and $k_2 = \frac{1}{6\pi^2} \simeq 0.01689$ of the perturbation theory to be developed in Section 4 (see Eq. (4.25)).

3.2 Discretisation of the integral equation for $P(r, E)$

To avoid the problems of the Monte Carlo method, we tried to numerically solve the integral equation (2.14) for $P(r, E)$. To this end the r -variable was discretised by taking 1000 values of r at the points $r_k = 2k/(2001 - 2k)$ for $1 \leq k \leq 1000$. The integral operator (2.14) then becomes a 1000×1000 matrix, and the stationary distribution can be obtained by simply iterating a linear system.

Figure 5 shows distributions $P(r, E)$ obtained that way. They are very similar to what was obtained by the MonteCarlo method, cfr. Figure 2.b–c. In Figure 6 we display the corresponding Lyapounov exponent $\gamma(E)$ and the density of states $\rho(E)$. The Lyapounov exponent is obtained simply by the discretised version of Eq. (2.15), and its derivatives are then calculated by replacing them by finite differences with a differentiation interval

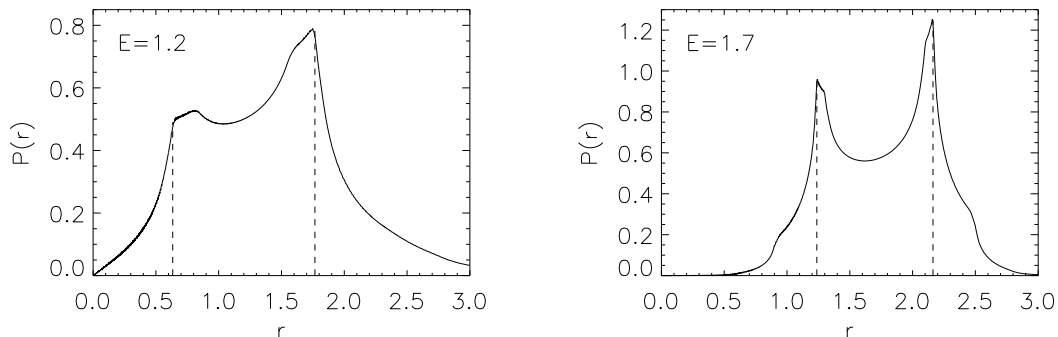


Figure 5: Invariant distributions $P(r, E)$ for energies $E = 1.2$ and 1.7 , obtained by discretisation of the integral equation (2.14).

$\Delta E = 0.025$. (This value results from a compromise: For smaller ΔE a complicated structure appears in the derivatives due to the discretisation of r , whereas a too large ΔE smears out details of $\rho(E)$.)

We see that both $\gamma(E)$ and $\rho(E)$ have essentially the same shapes as we have previously encountered in figure 4, using the Monte Carlo method. The irregularities which were visible in Figure 4.b have now disappeared in Figure 6.b. Moreover, the inset in Figure 6.a, showing the asymptotic approach towards the exact result (2.10), indicates that the accuracy of $\gamma(E)$ has been improved by roughly two orders of magnitude.

In the insets of Figures 4.a and 6.a, the difference $\gamma(E) - \log(E)$ seems to vanish at $E \simeq 1.8$. We believe that this difference is non-zero up to $E = 2$ but that it becomes very small ($\rho(E)$ has an essential singularity: it vanishes and all its derivatives vanish at $E = 2$). The argument that eigenstates exist up to $E = 2$ can be borrowed from the theory of Lifshitz tails [20, 21] in the Hermitian case: in a random sample, one can find arbitrarily large regions where $\theta_n \simeq \chi_n \simeq 0$.

4 Perturbation theory

In this section we develop a perturbation theory in powers of E to determine the invariant distribution $P(r, E)$ solution of Eq. (2.14). When this is known, we can obtain

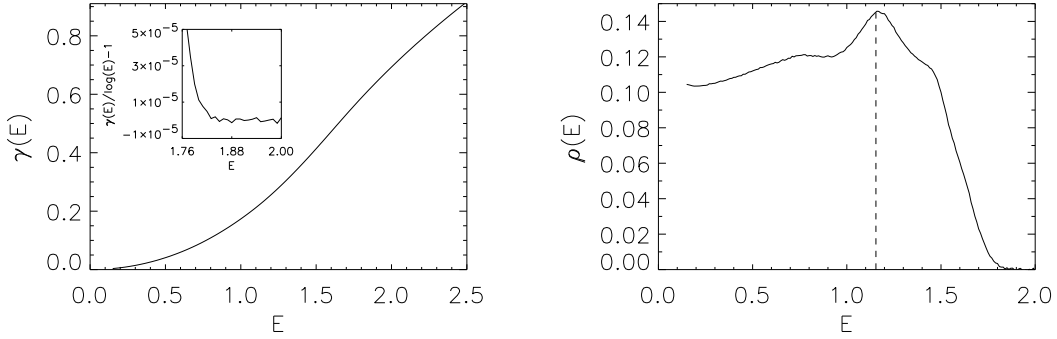


Figure 6: Lyapunov exponent $\gamma(E)$ and density of states $\rho(E)$ obtained by discretisation. The irregularities visible in Figure 4.b have now disappeared.

the corresponding perturbative series for $\gamma(E)$ from Eq. (2.15), and that of $\rho(E)$ from Eq. (2.9).

For $E = 0$ there are infinitely many solutions to Eq. (2.14). Namely, the iteration formula (2.12) reduces to

$$r_{n+1} = \frac{1}{r_n}, \quad (4.1)$$

and any distribution preverving the symmetry $r \leftrightarrow 1/r$ (*i.e.* such that $P(r, 0) = P(1/r, 0)/r^2$) is a solution. From Eq. (2.15) we thus immediately have

$$\gamma(E = 0) = 0. \quad (4.2)$$

On the other hand, for $|E| > 0$ the invariant distribution $P(r, E)$ is unique, as witnessed by the numerical results of Section 3. So the expansion in powers of E that we are going to develop presently is a degenerate perturbation theory, as there are many solutions when $E = 0$ and a single one, $P(r, E)$, when $E > 0$.

It is useful to analyse first the small- E expansion of the integral operator which appears in Eq. (2.14). Consider two distributions $\tilde{Q}(r)$ and $Q(r)$ related by

$$\tilde{Q}(r) = \int_0^{2\pi} \frac{d\varphi}{2\pi} \int_0^\infty ds Q(s) \delta\left(r - \left|\frac{1}{s} + Ee^{i\varphi}\right|\right). \quad (4.3)$$

When $E < r$, this can be rewritten (by integrating over s) as

$$\tilde{Q}(r) = \int_0^{2\pi} \frac{d\varphi}{2\pi} \frac{r^3 + rE^2 - 2rE^2 \sin^2 \varphi + 2rE \cos \varphi \sqrt{r^2 - E^2 \sin^2 \varphi}}{(r^2 - E^2)^2 \sqrt{r^2 - E^2 \sin^2 \varphi}} Q \left(\frac{E \cos \varphi + \sqrt{r^2 - E^2 \sin^2 \varphi}}{r^2 - E^2} \right). \quad (4.4)$$

Assuming $E \ll r$ the integrand can then be expanded as a power series in E , and after performing the integral over φ we find that

$$\begin{aligned} \tilde{Q}(r) &= \frac{1}{r^2} Q \left(\frac{1}{r} \right) + \frac{E^2}{4} \left[\frac{9}{r^4} Q \left(\frac{1}{r} \right) + \frac{7}{r^5} Q' \left(\frac{1}{r} \right) + \frac{1}{r^6} Q'' \left(\frac{1}{r} \right) \right] \\ &+ \frac{E^4}{64} \left[\frac{225}{r^6} Q \left(\frac{1}{r} \right) + \frac{351}{r^7} Q' \left(\frac{1}{r} \right) + \frac{149}{r^8} Q'' \left(\frac{1}{r} \right) + \frac{22}{r^9} Q^{(3)} \left(\frac{1}{r} \right) + \frac{1}{r^{10}} Q^{(4)} \left(\frac{1}{r} \right) \right] \\ &+ \frac{E^6}{2304} \left[\frac{11025}{r^8} Q \left(\frac{1}{r} \right) + \frac{25839}{r^9} Q' \left(\frac{1}{r} \right) + \frac{18261}{r^{10}} Q'' \left(\frac{1}{r} \right) + \frac{5382}{r^{11}} Q^{(3)} \left(\frac{1}{r} \right) + \right. \\ &\left. \frac{732}{r^{12}} Q^{(4)} \left(\frac{1}{r} \right) + \frac{45}{r^{13}} Q^{(5)} \left(\frac{1}{r} \right) + \frac{1}{r^{14}} Q^{(6)} \left(\frac{1}{r} \right) \right] + \mathcal{O}(E^8). \end{aligned} \quad (4.5)$$

We see that the effect of a non-zero energy is that $\tilde{Q}(r)$ is not just trivially related to $Q \left(\frac{1}{r} \right)$, but also depends on all the derivatives of Q . Quite remarkably, the above expansion can be written in a compact form valid to all orders. Defining the second order differential operator M by

$$M = \frac{d}{dr} r \frac{d}{dr} \frac{1}{r}, \quad (4.6)$$

the expansion of Eq. (4.4) to an arbitrary order in E can be written

$$\tilde{Q}(r) = \sum_{n=0}^{\infty} \frac{E^{2n}}{4^n (n!)^2} M^n \left[\frac{1}{r^2} Q \left(\frac{1}{r} \right) \right]. \quad (4.7)$$

It is straightforward to see that this agrees with the naïve expansion formula (4.5). The validity of Eq. (4.7) to an arbitrary order in E is established in Appendix B. Note that a simple change of variable $r \rightarrow 1/r$ transforms Eq. (4.7) into

$$\tilde{Q} \left(\frac{1}{r} \right) = \sum_{n=0}^{\infty} \frac{E^{2n}}{4^n (n!)^2} L^n \left[r^2 Q(r) \right], \quad (4.8)$$

where the operator L is defined by

$$L = r^2 \frac{d}{dr} r \frac{d}{dr} r. \quad (4.9)$$

Coming back to the invariant distribution $P(r, E)$, we see by combining Eqs. (4.7) and (4.8) that it satisfies

$$P(r, E) = \sum_{n=0}^{\infty} \left(\frac{E^2}{4} \right)^n \sum_{p=0}^n \frac{1}{[p! (n-p)!]^2} M^p \left[\frac{1}{r^2} L^{n-p} \left(r^2 P(r, E) \right) \right]. \quad (4.10)$$

If we look for a solution $P(r, E)$ which can be expanded as

$$P(r, E) = P_0(r) + \frac{E^2}{4}P_1(r) + \left(\frac{E^2}{4}\right)^2 P_2(r) + \dots, \quad (4.11)$$

we obtain by equating the two sides of Eq. (4.10), order by order in E , that

$$P_{m+1}(r) = \sum_{n=0}^{m+1} \sum_{p=0}^n \frac{1}{[p!(n-p)!]^2} M^p \left[\frac{1}{r^2} L^{n-p} \left(r^2 P_{m+1-n}(r) \right) \right]. \quad (4.12)$$

The term with $n = 0$ on the right-hand side is just $P_{m+1}(r)$, same as the left-hand side, so that $P_{m+1}(r)$ disappears from the equation. Therefore

$$\sum_{n=1}^{m+1} \sum_{p=0}^n \frac{1}{[p!(n-p)!]^2} M^p \left[\frac{1}{r^2} L^{n-p} \left(r^2 P_{m+1-n}(r) \right) \right] = 0. \quad (4.13)$$

Moving all but the two $n = 1$ terms, which are the only ones involving $P_m(r)$, to the right-hand side we arrive at the equation

$$\begin{aligned} M \left[(1 + r^4) P_m(r) \right] &= -M \sum_{n=2}^{m+1} \sum_{p=1}^n \frac{1}{[p!(n-p)!]^2} M^{p-1} \left[\frac{1}{r^2} L^{n-p} \left(r^2 P_{m+1-n}(r) \right) \right] \\ &\quad - M \sum_{n=2}^{m+1} \frac{1}{[n!]^2} r^2 L^{n-1} \left(r^2 P_{m+1-n}(r) \right). \end{aligned} \quad (4.14)$$

Note that an M operator has been factored out (by using the fact that $Lr^2 = r^2Mr^4$) from all the terms. Integrating over this, and shifting the summation variables, we finally find

$$\begin{aligned} (1 + r^4) P_m(r) &= A_m r \log r + B_m r - \sum_{n=1}^m \frac{1}{[(n+1)!]^2} r^2 L^n \left(r^2 P_{m-n}(r) \right) \\ &\quad - \sum_{n=1}^m \sum_{p=0}^n \frac{1}{[(p+1)!(n-p)!]^2} M^p \left[\frac{1}{r^2} L^{n-p} \left(r^2 P_{m-n}(r) \right) \right], \end{aligned} \quad (4.15)$$

where A_m and B_m are *a priori* arbitrary constants.

When $m = 0$ we find

$$P_0(r) = A_0 \frac{r \log r}{1 + r^4} + B_0 \frac{r}{1 + r^4}. \quad (4.16)$$

By inserting this into Eq. (4.7), with $Q(r)$ and $\tilde{Q}(r)$ replaced by $P(r, E)$, we see that for $P_0(r)$ to satisfy this equation to zeroth order in E , *i.e.* $P_0(r) = P_0(1/r)/r^2$, the constant A_0 should vanish, whereas B_0 could be arbitrary (the problem is linear and B_0 would be fixed by the normalisation of $P(r, E)$). This leads to $P_0(r) = B_0 r / (1 + r^4)$.

For the same reason, namely that $P(r, E)$ is the fixed point of Eq. (4.7) rather than the solution of Eq. (4.10) obtained by iterating Eq. (4.7) twice, one can show that $A_m = 0$ and B_m is arbitrary for all m . In fact, a non-zero B_m produces a contribution to $P_m(r)$ proportional to $P_0(r)$, and so one might as well choose $B_m = 0$ for all $m \neq 0$ by allowing B_0 to depend on E . In practise, then, all the $A_m = 0$ for $m \geq 0$, all the $B_m = 0$ for $m > 0$, and B_0 is an arbitrary function of E (which can be fixed by requiring that the distribution $P(r, E)$ be normalised).

In this way one arrives at

$$P(r, E) = B_0(E) \left[\frac{r}{1+r^4} + E^2 \left(\frac{r^3}{(1+r^4)^2} - \frac{4r^3}{(1+r^4)^4} \right) + \mathcal{O}(E^4) \right]. \quad (4.17)$$

The recursion (4.15) gives an explicit formula for the invariant distribution to *all orders* in powers of E . We now show how to produce the equivalent expansion for the Lyapunov exponent. First, it is easy to check by induction that all the $P_m(r)$ are finite sums of functions of the form

$$f_n(r) = \frac{r}{(1+r^4)^n} \quad \text{and} \quad g_n(r) = \frac{r^3}{(1+r^4)^n}. \quad (4.18)$$

Indeed, this is true for $m = 0$, and higher orders are generated from Eq. (4.15) by means of the operators M and L . These operators act on f_n and g_n as follows:

$$\begin{aligned} Mf_n &= 16n^2 g_{n+1} - 16n(n+1)g_{n+2}, \\ Mg_n &= 4(1-2n)^2 f_n - 32n^2 f_{n+1} + 16n(n+1)f_{n+2}, \\ Lf_n &= 4(1-2n)^2 g_n - 32n^2 g_{n+1} + 16n(n+1)g_{n+2}, \\ Lg_n &= 16(1-n)^2 f_{n-1} - 16(1-3n+3n^2)f_n + 48n^2 f_{n+1} - 16n(n+1)f_{n+2}. \end{aligned} \quad (4.19)$$

Applying Eq. (4.15) repeatedly, we have found the explicit expressions for the first seven orders of the (unnormalised) invariant distribution. We report the first few orders here, and defer the remaining ones to Appendix C.

$$\begin{aligned} P_0 &= f_1, \\ \frac{P_1}{4} &= g_2 - 4g_4, \\ \frac{P_2}{16} &= \frac{1}{2}f_2 + \frac{39}{2}f_3 - 22f_4 - 158f_5 + 320f_6 - 160f_7, \end{aligned}$$

$$\begin{aligned}
\frac{P_3}{64} &= \frac{1}{2}g_2 - \frac{673}{18}g_3 - \frac{131}{18}g_4 + \frac{4456}{3}g_5 - \frac{842}{3}g_6 - 21840g_7 \\
&+ 56520g_8 - 53760g_9 + 17920g_{10}.
\end{aligned} \tag{4.20}$$

In order to compute the contributions to $\gamma(E)$ and to the normalisation, one needs the following integrals

$$\begin{aligned}
I_n &= \int_0^\infty dr f_n(r), \\
J_n &= \int_0^\infty dr g_n(r), \\
K_n &= \int_0^\infty dr f_n(r) \log r, \\
L_n &= \int_0^\infty dr g_n(r) \log r.
\end{aligned} \tag{4.21}$$

Using (4.18), these are easily evaluated

$$\begin{aligned}
I_{n+1} &= \frac{2n-1}{2n}I_n \text{ with } I_1 = \frac{\pi}{4}, \\
J_n &= \frac{1}{4(n-1)}, \\
K_{n+1} &= \frac{2n-1}{2n}K_n - \frac{1}{4n}I_n \text{ with } K_1 = 0, \\
L_{n+1} &= \frac{n-1}{n}L_n - \frac{1}{4n}J_n \text{ with } L_2 = 0.
\end{aligned} \tag{4.22}$$

Combining all of this we arrive at the expansion

$$\gamma(E) = \frac{F(E)}{\pi G(E) + H(E)} \tag{4.23}$$

with

$$\begin{aligned}
F(E) &= \frac{1}{8}E^2 + \frac{5}{288}E^6 + \frac{43}{3600}E^{10} - \frac{2119}{235200}E^{14} + \mathcal{O}(E^{18}), \\
G(E) &= \frac{1}{4} + \frac{9}{256}E^4 + \frac{8333}{294912}E^8 + \frac{2624621}{56623104}E^{12} + \mathcal{O}(E^{16}), \\
H(E) &= -\frac{1}{12}E^2 - \frac{89}{15120}E^6 + \frac{1088497}{29937600}E^{10} + \frac{576717747329}{490377888000}E^{14} + \mathcal{O}(E^{18}).
\end{aligned} \tag{4.24}$$

It is worth noting that all the coefficients in the expansions of the functions F, G and H are rational. Equivalently,

$$\gamma(E) = \frac{1}{2\pi}E^2 + \frac{1}{6\pi^2}E^4 + \left(\frac{1}{18\pi^3} - \frac{1}{1152\pi}\right)E^6 + \left(\frac{1}{54\pi^4} - \frac{241}{20160\pi^2}\right)E^8$$

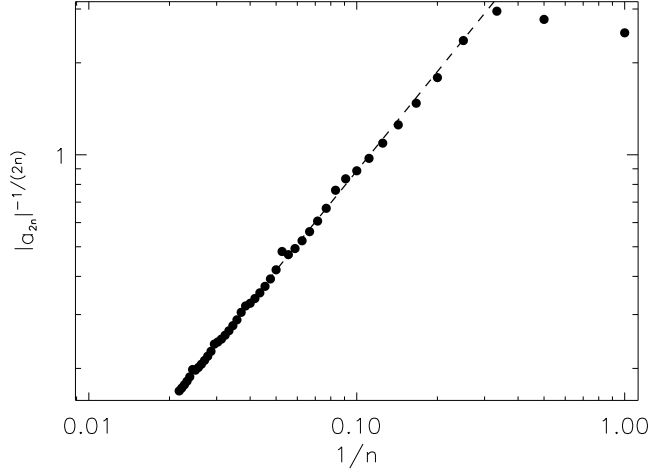


Figure 7: Log-log plot of $|a_{2n}|^{-1/(2n)}$ versus $1/n$.

$$\begin{aligned}
& + \left(\frac{1}{162\pi^5} - \frac{2857}{362880\pi^3} - \frac{31747}{3686400\pi} \right) E^{10} + \left(\frac{1}{486\pi^6} - \frac{1067}{272160\pi^4} - \frac{11849219}{127733760\pi^2} \right) E^{12} \\
& + \left(\frac{1}{1458\pi^7} - \frac{631}{362880\pi^5} - \frac{9755539001}{160944537600\pi^3} - \frac{530351263}{4161798144\pi} \right) E^{14} \\
& + \left(\frac{1}{4374\pi^8} - \frac{709}{979776\pi^6} - \frac{15094381}{502951680\pi^4} - \frac{128124296107}{53137244160\pi^2} \right) E^{16} + \mathcal{O}(E^{18}). \quad (4.25)
\end{aligned}$$

In this way we can in principle generate $\gamma(E)$ to any order. We calculated numerically the coefficients a_{2n} of the expansion of $\gamma(E)$

$$\gamma(E) = a_2 E^2 + a_4 E^4 + \dots + a_{2n} E^{2n} + \dots$$

up to $n = 46$ in order to estimate the radius of convergence of this series. In Figure 7 we show a log-log plot of $|a_{2n}|^{-1/(2n)}$ versus $1/n$. For $n > 10$ the data are well fitted by the form $|a_{2n}|^{-1/(2n)} \propto n^{-\nu}$ with $\nu \simeq 1.08$, shown as a dashed line on the figure. This result indicates rather convincingly that the large- n limit is zero, and thus that the radius of convergence vanishes. We therefore believe that our expansion is an asymptotic expansion.

5 Discussion

In this paper we have determined numerically the Lyapounov exponent $\gamma(E)$ and the density of states $\rho(E)$ of the one-dimensional non-Hermitian Schrödinger equation (1.2) when the phases θ_n and χ_n are uniformly distributed. We have also developed a method of expanding these quantities in powers of the energy E and obtained $\gamma(E)$ up to order E^{16} . Our procedure can be extended to obtain, in principle, an arbitrarily high order.

The expansion in powers of E is based on the expansion of the integral equation (2.14) satisfied by the invariant distribution $P(r, E)$. Since this expansion is in principle only valid for $E \ll r$, there is a possibility that the perturbation series for $\gamma(E)$ suffers from the fact that when we integrate over r , we use an expression valid for $r \gg E$ even in the neighborhood of $r = 0$. One cannot exclude for example that when r and E become comparable (and small), $P(r, E)$ becomes a scaling function of r/E . This could invalidate our expansion of $\gamma(E)$. However when we compared our expansion with the results of the simulation we found an excellent agreement for the first two terms and so it is possible that our expansion, *a priori* valid for $r \gg E$, remains valid down to $r = 0$.

Our numerical results show that the density of states vanishes outside a circle of radius $|E| = 2$, is non-zero inside this circle $|E| < 2$, and has a non-trivial shape with a pronounced maximum at an energy $E = 2/\sqrt{3}$. The analyticity of $\gamma(E)$ or of $\rho(E)$ at this energy remains an open problem. Another interesting question would be to predict how $\rho(E)$ vanishes at $E = 2$.

One could try to extend our approach to other situations, in particular to cases where the phases θ_n and χ_n have a non-uniform distribution [3]. In that case, the phase and the modulus of the ratio ψ_{n+1}/ψ_n are in general correlated and one should look for the invariant distribution $P(r, E)$ of the *complex variables* r_n and E . Still, the fact that $\gamma(E = 0) = 0$ would remain true, and one could try to expand the invariant distribution in powers of E and use the Thouless formula to calculate $\rho(E)$.

Acknowledgments

We would like to thank V. Hakim and L. Pastur for very useful and interesting discussions.

A Nature of the singularities of $P(r, E)$

In this Appendix we discuss the occurrence of singularities in the invariant measure $P(r, E)$ at the fixed point r_+ of the map $T_+(r) = E + \frac{1}{r}$, when one iterates the random map (2.12)

$$r_{n+1} = \left| \frac{1}{r_n} + Ee^{i\varphi_n} \right|, \quad (\text{A.1})$$

with uniformly distributed φ_n between 0 and 2π .

We believe that the apparent singularities in $P(r, E)$ seen in Figure 2 are due to events where several successive r_n are close to the fixed point r_+ , and that the nature of the singularity can be understood by analysing only the neighbourhood of r_+ .

In physical terms, there is a competition between the deterministic part of the map $T_+(r)$ which tries to concentrate the distribution on its attractive fixed point r_+ , and the noise due to φ_n which tends to broaden the distribution. To analyse the neighbourhood of r_+ , we consider the linearised problem

$$s_{n+1} = -as_n + t_n, \quad (\text{A.2})$$

where $a \in]0, 1[$ is a fixed slope, and t_n is a random positive number. The variable s_n represents the difference $r_+ - r_n$, when this difference is small. By expanding Eq. (A.1) to second order in φ_n , it is seen that for Eqs. (A.1) and (A.2) to be equivalent in the neighbourhood of r_+ , one should choose

$$\begin{aligned} a &= -T'_+(r_+) = \frac{E^2 + 2 - E\sqrt{E^2 + 4}}{2}, \\ t_n &= \frac{E}{2(Er_+ + 1)} \varphi_n^2. \end{aligned} \quad (\text{A.3})$$

The essential feature of the distribution of t_n is that all the t_n are positive and that the distribution $Q(t)$ of t_n diverges as $Q(t) \sim t^{-1/2}$ as $t \rightarrow 0$. If we iterate (A.2) numerically for $E = 1.7$, that is for $a = 0.213851 \dots$, we recover at $s = 0$ a singularity (see Figure 8.a) which resembles the one seen on Figure 2.c. Actually, the two distributions are approximately mirror images near their respective fixed points, but this is due to the fact that $s_n \simeq r_+ - r_n$ rather than $s_n \simeq r_n - r_+$.

Trying to analyse the nature of this singularity, we see from Eq. (A.2) that s_n can be written as

$$s_n = t_{n-1} - at_{n-2} + a^2t_{n-3} - a^3t_{n-4} + a^4t_{n-5} - \dots \quad (\text{A.4})$$

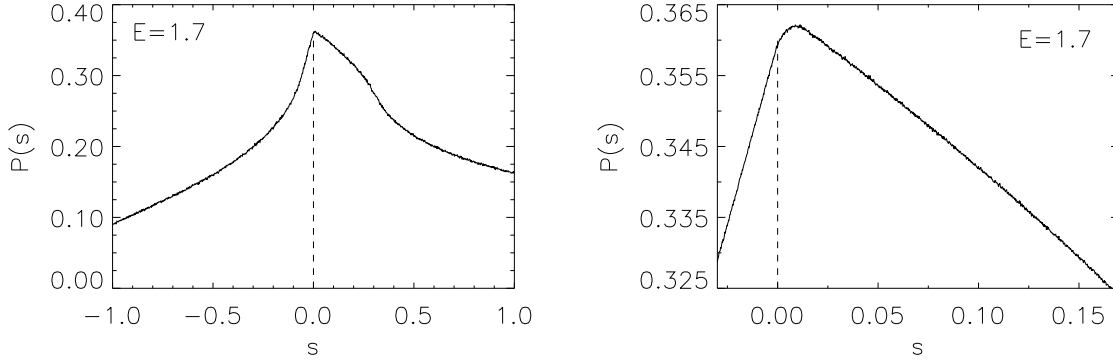


Figure 8: Invariant distribution of s_n for the linearised problem defined by Eqs. (A.2)–(A.3), here with $E = 1.7$. The magnification (obtained with $N = 10^{11}$ iterations) shows that there is in fact no singularity at $s = 0$.

or as

$$s_n = y_n - ay'_n, \quad (\text{A.5})$$

where y_n and y'_n are two positive independent and equally distributed random variables of the form

$$\begin{aligned} y_n &= \tau_n + a^2\tau_{n-1} + a^4\tau_{n-2} + a^6\tau_{n-3} + \dots, \\ y'_n &= \tau'_n + a^2\tau'_{n-1} + a^4\tau'_{n-2} + a^6\tau'_{n-3} + \dots. \end{aligned} \quad (\text{A.6})$$

All the τ_n and the τ'_n are independent and distributed according to the same distribution $Q(t)$ as for the t_n .

Let us first consider the case where s_n is still given by Eq. (A.5) but where the distribution $\pi(y)$ of the *positive* variables y is arbitrary. Using Eq. (A.5) one can show that the distribution $P(s)$ of s is given by

$$P(s) = \int_0^\infty dy \pi(ay + s) \pi(y) \quad \text{for } s > 0, \quad (\text{A.7})$$

$$P(s) = \int_0^\infty dy \pi(ay) \pi\left(y - \frac{s}{a}\right) \quad \text{for } s < 0. \quad (\text{A.8})$$

One can calculate the successive derivatives with respect to s at $s = 0$, and one obtains for the n^{th} derivative

$$P^{(n)}(0_+) = \int_0^\infty dy \pi^{(n)}(ay) \pi(y), \quad (\text{A.9})$$

$$P^{(n)}(0_-) = \left(\frac{-1}{a}\right)^n \int_0^\infty dy \pi(ay) \pi^{(n)}(y). \quad (\text{A.10})$$

If we assume that $\pi(y)$ and its first $\left[\frac{n+1}{2}\right]$ derivatives vanish at the origin, and as $y \rightarrow \infty$, it is easy to see by integration by parts that Eqs. (A.9) and (A.10) coincide, so that $P(s)$ has at least n derivatives at 0.

We are now going to argue that since y_n is given by Eq. (A.6), its stationary distribution $\pi(y)$ vanishes at $y = 0$ as well as all its derivatives. To see this, let us consider the generating function $\langle e^{-\beta y} \rangle$ of y . From Eq. (A.6) one has

$$\langle e^{-\beta y} \rangle = \prod_{n=0}^{\infty} \left[\int_0^\infty dt Q(t) e^{-\beta t a^{2n}} \right]. \quad (\text{A.11})$$

Because $Q(t) \sim t^{-1/2}$ for small t , one has for large β

$$\int_0^\infty dt Q(t) e^{-\beta t} \simeq \frac{B}{\beta^{1/2}}. \quad (\text{A.12})$$

For large β , one has $\langle e^{-\beta y} \rangle \simeq \langle e^{-\beta a^2 y} \rangle$ and one finds that to leading order

$$\log \left[\langle e^{-\beta y} \rangle \right] \simeq \frac{1 \log^2 \beta}{8 \log a}. \quad (\text{A.13})$$

We see that $\langle e^{-\beta y} \rangle$ vanishes faster (as $\log a < 0$) than any negative power of β as $\beta \rightarrow \infty$. As a consequence $\pi(y)$ and all its derivatives vanish at $y = 0$.

Therefore we can conclude that all the derivatives of the distribution $P(s)$ are continuous at $s = 0$. This is confirmed by a magnification of the small- s region, as seen in Figure 8.b, where the rounding of $P(s)$ at $s = 0$ becomes visible.

Coming back to the stationary distribution $P(r, E)$, we observe the same rounding of the apparent singularity at r_+ (see Figure 3).

B Justification of Eq. (4.7)

Imagine that s is a random positive variable distributed according to some given distribution $Q(s)$ and let r be given by

$$r = \left| \frac{1}{s} + E e^{i\varphi} \right|, \quad (\text{B.1})$$

where φ is uniformly distributed between 0 and 2π . We want to show that the distribution $\tilde{Q}(r)$ of r can be written as in Eq. (4.7):

$$\tilde{Q}(r) = \sum_{n=0}^{\infty} \frac{E^{2n}}{4^n (n!)^2} M^n \left[\frac{1}{r^2} Q \left(\frac{1}{r} \right) \right], \quad (\text{B.2})$$

where

$$M = \frac{d}{dr} r \frac{d}{dr} \frac{1}{r} \quad (\text{B.3})$$

Let us assume for simplicity that all (positive and negative) moments of $Q(s)$ exist. By taking the $(2p)^{\text{th}}$ power of Eq. (B.1) and by averaging over φ , one can see that

$$\int_0^{\infty} dr r^{2p} \tilde{Q}(r) = \sum_{n=0}^p \frac{[p!]^2}{[n!]^2 [(p-n)!]^2} E^{2n} \int_0^{\infty} ds \frac{1}{s^{2p-2n}} Q(s). \quad (\text{B.4})$$

We see that for Eqs. (B.2) and (B.4) to be equivalent, one simply need to show that

$$\frac{1}{4^n} \int_0^{\infty} dr r^{2p} M^n \left[\frac{1}{r^2} Q \left(\frac{1}{r} \right) \right] = \frac{[p!]^2}{[(p-n)!]^2} \int_0^{\infty} ds \frac{1}{s^{2p-2n}} Q(s). \quad (\text{B.5})$$

For $n = 0$ this is an obvious identity, and for $n > 0$ it can be established by induction, using integrations by parts.

C Higher orders of $P(r, E)$

Here we list the higher order terms of $P(r, E)$, obtained from Eq. (4.15), expressed in terms of the elementary functions f_n and g_n . These higher order terms are used together with Eq. (4.20) to obtain the expansion (4.23) for the Lyapunov exponents.

$$\begin{aligned} \frac{P_4}{4^4} &= \frac{221}{8} f_2 + \frac{16295}{72} f_3 - \frac{94193}{18} f_4 - 25803 f_5 + \frac{2529101}{9} f_6 + \frac{2619745}{9} f_7 \\ &- \frac{22135892}{3} f_8 + \frac{77875796}{3} f_9 - 43988480 f_{10} + 40636800 f_{11} - 19712000 f_{12} \\ &+ 3942400 f_{13}, \end{aligned} \quad (\text{C.1})$$

$$\begin{aligned} \frac{P_5}{4^5} &= -\frac{413}{72} g_2 - \frac{370801}{648} g_3 + \frac{11887541}{3240} g_4 + \frac{34137437}{135} g_5 - \frac{76908091}{135} g_6 \\ &- \frac{174769499}{9} g_7 + \frac{684150977}{9} g_8 + \frac{1394447776}{3} g_9 - \frac{38774321284}{9} g_{10} \\ &+ 14632026816 g_{11} - 27725662640 g_{12} + 31886412800 g_{13} - 22180787200 g_{14} \\ &+ 8610201600 g_{15} - 1435033600 g_{16}, \end{aligned} \quad (\text{C.2})$$

$$\begin{aligned}
\frac{P_6}{4^6} &= \frac{132619}{288}f_2 + \frac{55698437}{2592}f_3 - \frac{1031521993}{1080}f_4 - \frac{10179687761}{1080}f_5 + \frac{76720899118}{405}f_6 \\
&+ \frac{166044285683}{270}f_7 - \frac{2068679706428}{135}f_8 + \frac{3096140849561}{135}f_9 + \frac{1697546657546}{3}f_{10} \\
&- 4380421880262f_{11} + \frac{147448995026264}{9}f_{12} - 38217908241192f_{13} \\
&+ \frac{179597752851712}{3}f_{14} - \frac{192990668440960}{3}f_{15} + 46970084761600f_{16} \\
&- 22329532825600f_{17} + 6245266227200f_{18} - 780658278400f_{19} \tag{C.3}
\end{aligned}$$

$$\begin{aligned}
\frac{P_7}{4^7} &= -\frac{288203}{2592}g_2 - \frac{1354843111}{23328}g_3 + \frac{815716196107}{583200}g_4 + \frac{16419260711323}{170100}g_5 \\
&- \frac{207216071509033}{340200}g_6 - \frac{113911389465407}{5670}g_7 + \frac{579469587812377}{5670}g_8 \\
&+ \frac{677054300749364}{405}g_9 - \frac{1078075200453799}{81}g_{10} - \frac{324458646218758}{9}g_{11} \\
&+ \frac{8114117353035130}{9}g_{12} - \frac{50273274830679712}{9}g_{13} + \frac{180446654936149976}{9}g_{14} \\
&- \frac{433731592050615872}{9}g_{15} + \frac{735643743703812320}{9}g_{16} - \frac{298906446014525440}{3}g_{17} \\
&+ \frac{261230176431411200}{3}g_{18} - 53361562052198400g_{19} + 21803255983308800g_{20} \\
&- 5339702624256000g_{21} + 593300291584000g_{22}. \tag{C.4}
\end{aligned}$$

References

- [1] N. Hatano and D. R. Nelson, Phys. Rev. Lett. **77**, 570 (1996).
- [2] N. Hatano and D. R. Nelson, Phys. Rev. B **56**, 8651 (1997).
- [3] J. Feinberg and A. Zee, preprint cond-mat/9706218
- [4] D. R. Nelson and N. M. Shnerb, Phys. Rev. E **58**, 1383 (1998).
- [5] I. Y. Goldsheid and B. A. Khoruzhenko, Phys. Rev. Lett. **80**, 2897 (1998).
- [6] P. W. Brouwer, P. G. Silvestrov and C. W. J. Beenakker, Phys. Rev. B **56**, R4333 (1997).
- [7] A. Zee, Physica A **254**, 300 (1998).
- [8] N. Hatano, Physica A **254**, 317 (1998).
- [9] K. B. Efetov, Phys. Rev. Lett. **79** 491 (1997).
- [10] J. Feinberg and A. Zee, Nucl. Phys. B **504** 579 (1997).
- [11] E. Brézin and A. Zee, Nucl. Phys. B **509**, 599 (1998).
- [12] C. Mudry, P. W. Brouwer, B. I. Halperin, V. Gurarie and A. Zee, Phys. Rev. B **58**, 13539 (1998).
- [13] F. J. Dyson, Phys. Rev. **92**, 1331 (1953).
- [14] H. Schmidt, Phys. Rev. **105**, 425 (1957).
- [15] M. Kappus and F. Wegner, Z. Phys. B **45**, 15 (1981).
- [16] B. Derrida and E. Gardner, J. Physique **45**, 1283 (1984).
- [17] D. J. Thouless, J. Phys. C **5**, 77 (1972).
- [18] H. Furstenberg, Trans. Am. Math. Soc. **68**, 377 (1963).
- [19] L. A. Pastur, private communication.
- [20] I. M. Lifshitz, S. A. Gredeskul and L. A. Pastur, *Introduction to the theory of disordered systems*, Wiley, New York 1988.
- [21] L. A. Pastur and A. Figotin, *Spectra of random and almost periodic operators*, Springer Verlag, Berlin 1992.